

# Influence of the Concentrations of Aluminium and Silicon in the Liquid Phase on the Growth Kinetics of Zeolite A and X Microcrystals

Sanja Bosnar, Josip Bronić, Ivan Krznarić, and Boris Subotić\*

*Rudjer Bošković Institute, Laboratory for the Synthesis of New Materials, Division of Material Chemistry, P.O. Box 180, 10002 Zagreb, Croatia*

RECEIVED DECEMBER 10, 2003; REVISED MARCH 11, 2004; ACCEPTED MAY 10, 2004

Kinetics of the crystal growth of zeolites A and X was measured during their crystallization, at 80 °C, from an amorphous aluminosilicate precursor dispersed in a 1.4 M NaOH solution containing different amounts of dissolved  $\text{NaAlO}_2$  or  $\text{Na}_2\text{SiO}_3$ . The crystallization pathway and fractions of zeolites A and X in the crystalline end product strongly depend on the composition of the liquid phase of the crystallizing system. Analyses of the changes of the concentrations of aluminium,  $c_{\text{Al}}$ , and of silicon,  $c_{\text{Si}}$ , in the liquid phase as well as of the dimension,  $L_m$ , of the largest crystals of zeolites A and X during crystallization, have shown that the growth rate of zeolite A crystals is size-independent, and that the growth is governed by the reaction of monomeric and/or low-molecular aluminate, silicate and aluminosilicate anions from the liquid phase on the surfaces of growing zeolite crystals. Influence of the composition of the liquid phase of the crystallizing system on the course of crystallization process and on the growth rates of zeolite A and zeolite X crystals are discussed in terms of the possible distribution of aluminate, silicate and/or aluminosilicate anions in the liquid phase.

*Keywords*  
zeolite A  
zeolite X  
aluminate  
silicate  
crystallization  
crystal growth

## INTRODUCTION

There is abundant experimental evidence that the rate,  $R_g$ , of the crystal growth of zeolites depends on the concentrations of both silicon and aluminium in the liquid phase of the crystallizing system,<sup>1–13</sup> *i.e.*,

$$R_g = dL/dt_c = k_g f(c) = k_g f(c_{\text{Al}}, c_{\text{Al}}^*, c_{\text{Si}}, c_{\text{Si}}^*) \quad (1)$$

where  $L$  is the crystal size at crystallization time  $t_c$ ,  $k_g$  is the rate constant of linear crystal growth,  $f(c)$  is the concentration factor,<sup>1,14–18</sup>  $c_{\text{Al}}$  and  $c_{\text{Si}}$  are the concentrations of aluminium and silicon in the liquid phase during crystallization, and  $c_{\text{Al}}^*$  and  $c_{\text{Si}}^*$  are the concentrations of alu-

minium and silicon in the liquid phase, which correspond to the solubility of zeolite under the given crystallization conditions. The linear relationship between the size-independent crystal growth and the concentration factor,  $f(c)$ ,<sup>1,3–5,9–13,18</sup> can be explained by the Davies and Jones model of crystal growth and dissolution,<sup>19,20</sup> which predicts formation of a monolayer of solvated ions with a constant composition of the surface of growing/dissolving crystals. According to this model, the rate of crystal growth of zeolites is proportional to the product of the fluxes,  $F_{\text{Al}} = (c_{\text{Al}} - c_{\text{Al}}^*)$ , and  $F_{\text{Si}} = (c_{\text{Si}} - c_{\text{Si}}^*)$  of aluminate and silicate anions participating in the surface reaction, and thus:<sup>10–13,18,21</sup>

\* Author to whom correspondence should be addressed. (E-mail: [subotic@rudjer.irb.hr](mailto:subotic@rudjer.irb.hr))

$$dL/dt_c = k_g f(c) = k_g F_{Al} (F_{Si})^r = k_g (c_{Al} - c_{Al}^*)(c_{Si} - c_{Si}^*)^r \quad (2)$$

where  $r$  is the Si/Al mole ratio of the crystallized zeolite.<sup>11,13,18</sup>

Based on the influence of various factors on the  $k_g$  value,<sup>1,10–13,18</sup> it is beyond dispute that the  $k_g$  value is influenced not only by the kinetic energies of the reactive aluminate, silicate and/or aluminosilicate anions, but also by their distributions with respect to size, charge and structure. Since these distributions depend on the concentrations of silicon and aluminium in the liquid phase and on the system alkalinity of,<sup>22–26</sup> the rate of crystal growth depends on the concentrations of aluminium and silicon in the liquid phase not only by the relationship formally represented by Eq. (2), but also by the dependence of the  $k_g$  value on the concentration-dependent properties (size, charge and structure) of the reactive species in the liquid phase. Although, as already stated, it is known that the growth rate of zeolite microcrystals is influenced by the concentrations of silicon and aluminium in the liquid phase in accordance with Eq. (2),<sup>10–13,18,21</sup> the influence of these factors on the rate constant  $k_g$  is not known. Hence, the objective of this work is to investigate the influence of the concentrations  $c_{Al}$  and  $c_{Si}$  of aluminium and silicon in the liquid phase of specially designed crystallizing systems<sup>11,18,21</sup> on the kinetics of the crystal growth of zeolite A and zeolite X microcrystals, taking into consideration the influence of the concentration-dependent properties of the reactive species in the liquid phase on the value of  $k_g$ .

## EXPERIMENTAL

Water suspension containing 16 % (mass fraction,  $w$ ) of X-ray amorphous aluminosilicate precursor ( $1.03 \text{ Na}_2\text{O} \cdot \text{Al}_2\text{O}_3 \cdot$

$2.63 \text{ SiO}_2 \cdot 2.66 \text{ H}_2\text{O}$ ) was prepared by the procedure described previously.<sup>11,21</sup> A hundred ml of the suspension was poured into a stainless-steel reaction vessel and then warmed up at 80 °C. The reaction vessel was provided with a thermostated jacket and fitted with a water-cooled reflux condenser and thermometer. When the suspension was thermostated at the reaction temperature (80 °C), 100 ml of alkaline solution (see Table I) thermostated at 80 °C was quickly added to the suspension. Thus prepared reaction mixtures contained 8 % ( $w$ ) of the solid phase ( $1.03 \text{ Na}_2\text{O} \cdot \text{Al}_2\text{O}_3 \cdot 2.38 \text{ SiO}_2 \cdot 1.66 \text{ H}_2\text{O}$ ) dispersed in the solutions having the chemical compositions as shown in Table I. The reaction mixtures were heated at 80 °C under stirring with a Teflon-coated magnetic bar driven by a magnetic stirrer. At various times,  $t_c$ , after the onset of the crystallization process, aliquots of the reaction mixture were drawn off to prepare the samples for analysis. The moment when the alkaline solution was added to the previously prepared suspension was taken as zero time of the crystallization process.

Aliquots of the reaction mixture drawn off at the given crystallization times,  $t_c$ , were poured into cuvettes and were centrifuged to stop the crystallization process and to separate the solid from the liquid phase. Part of the clear liquid phase (supernatant) was diluted with distilled water to the concentration ranges available for measuring the aluminium and silicon concentrations by atomic absorption spectroscopy. The remaining supernatant was carefully removed without disturbing the solid phase (sediment). After the supernatant was removed, the solid phase was redispersed in distilled water and centrifuged repeatedly. The procedure was repeated until the pH value of the liquid phase above the sediment was 9. The wet washed solids were dried overnight at 105 °C, cooled in a desiccator with silicagel and pulverized in an agate mortar. The powdered solids were used for determination of the fraction,  $f_c$ , of crystallized zeolite(s), for measurements of the particle size distribution and the size of the largest crystals.

TABLE I. Scheme of the preparation of crystallizing systems and chemical compositions of the liquid phases of the crystallizing systems

System	Preparation <sup>(a)</sup>		Starting composition of the liquid phase <sup>(b)</sup>
	Aluminosilicate suspension <sup>(c)</sup>	Alkaline solution	
Ø	16 % amorphous aluminosilicate	2.8 mol dm <sup>-3</sup> NaOH	0.7 mol dm <sup>-3</sup> Na <sub>2</sub> O
A1	16 % amorphous aluminosilicate	2.8 mol dm <sup>-3</sup> NaOH + 0.092 mol dm <sup>-3</sup> NaAlO <sub>2</sub>	0.723 mol dm <sup>-3</sup> Na <sub>2</sub> O + 0.023 mol dm <sup>-3</sup> Al <sub>2</sub> O <sub>3</sub>
A2	16 % amorphous aluminosilicate	2.8 mol dm <sup>-3</sup> NaOH + 0.18 mol dm <sup>-3</sup> NaAlO <sub>2</sub>	0.745 mol dm <sup>-3</sup> Na <sub>2</sub> O + 0.045 mol dm <sup>-3</sup> Al <sub>2</sub> O <sub>3</sub>
A3	16 % amorphous aluminosilicate	2.8 mol dm <sup>-3</sup> NaOH + 0.272 mol dm <sup>-3</sup> NaAlO <sub>2</sub>	0.768 mol dm <sup>-3</sup> Na <sub>2</sub> O + 0.068 mol dm <sup>-3</sup> Al <sub>2</sub> O <sub>3</sub>
S1	16 % amorphous aluminosilicate	2.8 mol dm <sup>-3</sup> NaOH + 0.068 mol dm <sup>-3</sup> Na <sub>2</sub> SiO <sub>3</sub>	0.734 mol dm <sup>-3</sup> Na <sub>2</sub> O + 0.034 mol dm <sup>-3</sup> SiO <sub>2</sub>
S2	16 % amorphous aluminosilicate	2.8 mol dm <sup>-3</sup> NaOH + 0.136 mol dm <sup>-3</sup> Na <sub>2</sub> SiO <sub>3</sub>	0.768 mol dm <sup>-3</sup> Na <sub>2</sub> O + 0.068 mol dm <sup>-3</sup> SiO <sub>2</sub>
S3	16 % amorphous aluminosilicate	2.8 mol dm <sup>-3</sup> NaOH + 0.204 mol dm <sup>-3</sup> Na <sub>2</sub> SiO <sub>3</sub>	0.802 mol dm <sup>-3</sup> Na <sub>2</sub> O + 0.102 mol dm <sup>-3</sup> SiO <sub>2</sub>

<sup>(a)</sup> 100 ml of aluminosilicate water suspension + 100 ml of alkaline solution.

<sup>(b)</sup> Na<sub>2</sub>O, Al<sub>2</sub>O<sub>3</sub> and SiO<sub>2</sub> exist in their soluble forms (Na<sup>+</sup>, OH<sup>-</sup>, aluminate anions, silicate anions).

<sup>(c)</sup> Mass fractions,  $w$ .

The X-ray spectra of the samples were taken with a Philips diffractometer (Cu-K $\alpha$  radiation) in the corresponding region of Bragg's angles. The mass fractions of crystalline and amorphous phases were calculated by a combined method<sup>27</sup> using the integral value of the broad amorphous peak ( $2\theta = 17\text{--}39^\circ$ ) and the corresponding sharp peaks of crystalline phase(s).

Concentrations of sodium, aluminium and silicon in the solutions obtained by dissolving the calcined samples and the ones obtained by dilution of the liquid phases separated from the reaction mixtures at various crystallization times,  $t_c$ , were measured using a Perkin-Elmer 3030B atomic absorption spectrometer.

The size of the largest crystals in the solid samples drawn off the reaction mixture at various crystallization times,  $t_c$ , were determined by the method proposed by Zhdanov,<sup>5</sup> using optical microscopy.

The particle size distribution curves of the crystalline end products were determined with a Malvern's »Mastersizer X LB« laser light scattering particle size analyzer. Before measurement, powdered samples were dispersed in demineralized water by ultrasonic waves (min. 30 min), and the instrument was calibrated using the standard latex solution. The performed measuring procedure is the standard procedure for wet polydispersed samples within the optimal instrument setting (100 mm lens focus, 50 % power of stirring and 50 % power of ultrasonic waves). At least 5 scans of each sample were recorded and all were taken under the same conditions.

## RESULTS AND DISCUSSION

Figure 1 shows that an »excess« of aluminium in the liquid phase (systems: A1,  $\Delta$ ; A2,  $\circ$ ; and A3,  $\square$ ) increases both the rate of crystallization (Figure 1a) and the rate of the crystal growth of zeolite A (Figure 1b) relative to the reference system (system  $\emptyset$ ,  $\nabla$ ). However, either the rate of crystallization (Figure 1a) or the linear rate  $dL_m/dt_c = R_g$  of crystal growth (Table II; solid curves in Figure 1b) are not influenced markedly by the degree of the »excess« of aluminium in the liquid phase. On the other hand, the increase in the silicon concentration (»excess«) in the liquid phase (systems: S1,  $\bullet$ ; S2,  $\blacktriangle$ ; and S3,  $\blacksquare$ ) causes two effects: (i) a decrease of the rates of both crystallization (Figure 1a) and crystal growth (Figure 1b) of zeolite A in systems S1 and S2, and (ii) a simultaneous crystallization of zeolites A (Figure 1a) and X (Figure 1c). While zeolite X did not crystallize at the lowest »excess« of silicon in the liquid phase (system S1, Figure 1a), zeolite X is dominant phase crystallized at an increased concentration (»excess«) of silicon in the liquid phase (systems S2 and S3, Figure 1c). Moreover, zeolite X was the only product crystallized in system S3 (Figure 1c).

Since all the aluminosilicate gel precursors were prepared in the same way (see Experimental), one can expect all the precursors to have the same number and dis-

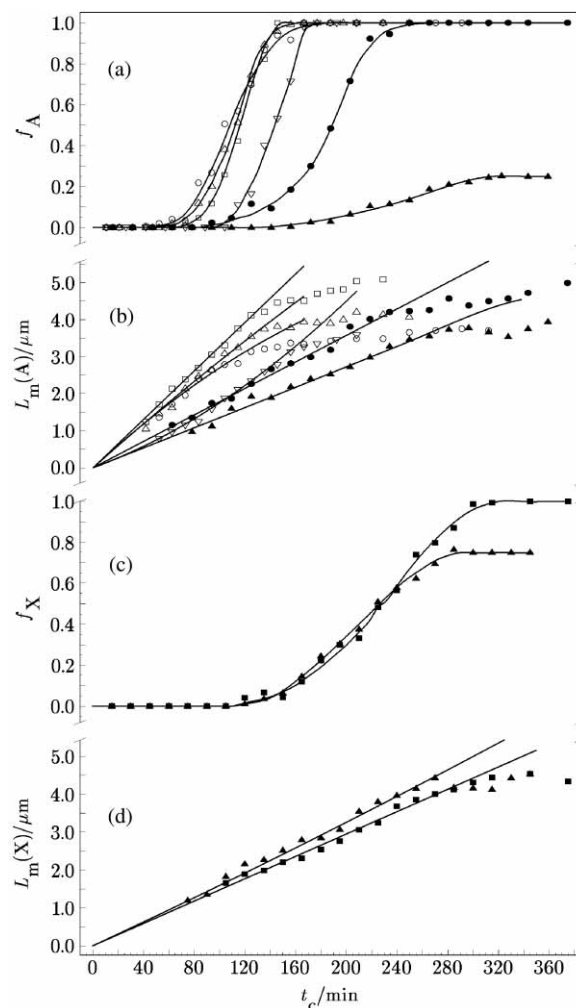


Figure 1. Changes in (a) fractions  $f_A$  of zeolite A and (c)  $f_X$  of zeolite X, (b) size  $L_m(A)$  of the largest crystals of zeolite A, and (d) size  $L_m(X)$  of the largest crystals of zeolite X during crystallization from systems  $\emptyset$  ( $\nabla$ ), A1 ( $\Delta$ ), A2 ( $\circ$ ), A3 ( $\square$ ), S1 ( $\bullet$ ), S2 ( $\blacktriangle$ ), and S3 ( $\blacksquare$ ). The solid straight lines in Figures (b) and (d) represent the changes in the size of the largest zeolite crystals calculated by Eq. (6).

TABLE II. Numerical values of the rate constants  $R_g$  of the growth of zeolites A and X crystals in systems  $\emptyset$ , A1, A2, A3, S1, S2 and S3

System	$R_g(A) / \mu\text{m min}^{-1}$	$R_g(X) / \mu\text{m min}^{-1}$
A3	0.019	–
A2	0.028	–
A1	0.029	–
$\emptyset$	0.034	–
S1	0.019	–
S2	0.0034	0.017
S3	–	0.015

tribution of nuclei through their matrixes.<sup>1,4,18,21,28,29</sup> In this case, although the rates of nucleation, crystal growth and crystallization largely depend on the crystallization conditions, these factors do not affect particulate properties of the crystalline end products, as defined by the prin-

TABLE III. Numerical values of the average size  $\bar{L}$  and specific number  $\bar{N}$  of zeolite crystals in the crystalline end products crystallized from systems  $\emptyset$ , A1, A2, A3, S1, S2 and S3

System	$\bar{L} / \mu\text{m}$	$\bar{N} / \text{g}^{-1}$
$\emptyset$	1.03	$1.65 \times 10^{11}$
A1	1.07	$1.72 \times 10^{11}$
A2	1.09	$1.42 \times 10^{11}$
A3	1.09	$1.76 \times 10^{11}$
S1	1.17	$1.43 \times 10^{11}$
S2	1.03	$1.89 \times 10^{11}$
S3	1.12	$1.45 \times 10^{11}$

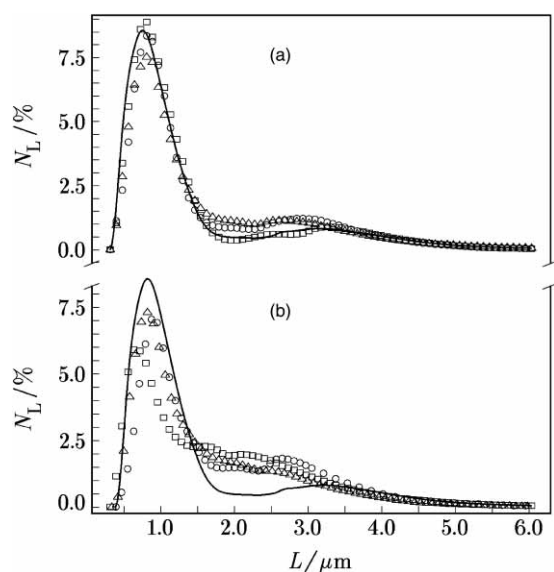


Figure 2. Crystal size distributions of the crystalline end products obtained by crystallization of zeolite from systems: (a) A1 (O), A2 (Δ) and A3 (□) and (b) S1 (O), S2 (Δ) and S3 (□). Solid curves in Figures (a) and (b) represent the crystal size distribution of the crystalline end product (zeolite A) obtained by its crystallization from system  $\emptyset$ .  $N_L$  is the number frequency of zeolite A crystals having size  $L$ .

principle of the »memory effect« of amorphous aluminosilicate precursors.<sup>28–31</sup> In this context, the insensitivity of the particulate properties (crystal size distribution; Figure 2, average size  $\bar{L}$  and specific number  $\bar{N}$  of zeolite A crystals; see Table III) of the crystalline end products to the excess of aluminate and silicate anions, respectively, in the liquid phase is expected in accordance with the »memory effect« of amorphous aluminosilicate precursors. Here, it is particularly interesting that the crystal size distribution of a mixture of zeolites A and X (system S2) and zeolite X alone (system S3) is very close to the crystal size distribution of zeolite A crystallized from systems  $\emptyset$ , A1, A2, A3 and S1 (see Figure 2). This means that both zeolite A and X are formed by the growth of the same »type« of nuclei, and that the type of zeolite crystallized depends on the composition of the liquid phase of the system ( $c_{\text{Al}}$ ,  $c_{\text{Si}}$  and  $c_{\text{Si}}/c_{\text{Al}}$ ) rather than on the

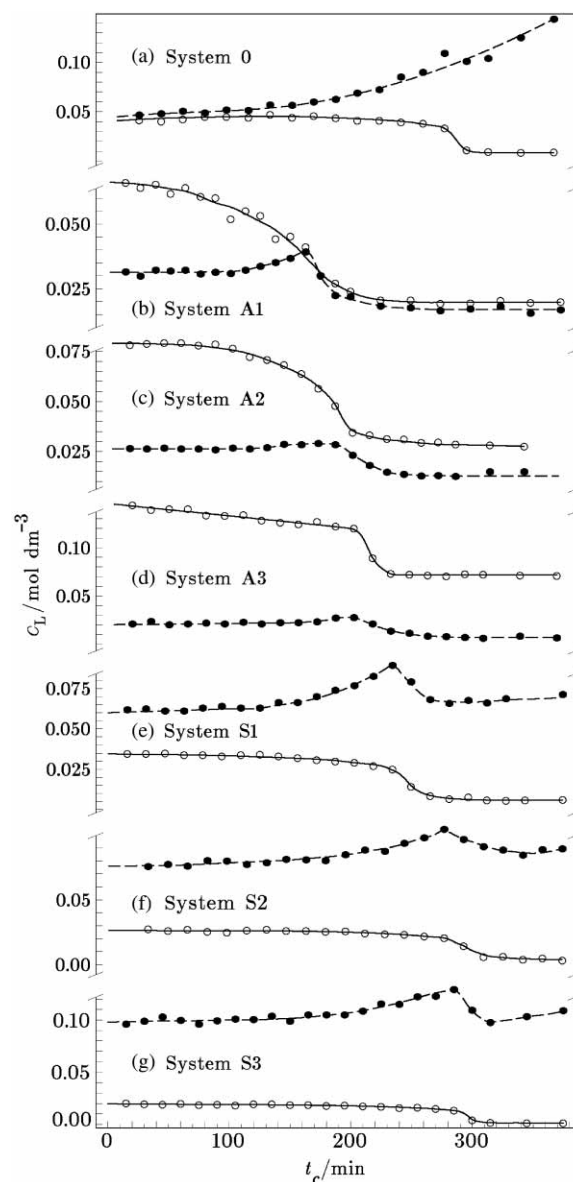


Figure 3. Changes in concentrations  $c_L = c_{\text{Al}}$ , of aluminum (O, solid curve) and  $c_L = c_{\text{Si}}$ , of silicon (●, dashed curve) in the liquid phase during hydrothermal treatment of systems  $\emptyset$ , A1, A2, A3, S1, S2 and S3 at 80 °C.

»structure« of nuclei formed in the gel matrix. This finding is in agreement with the previously observed co-crystallization of zeolites A and X.<sup>1,18,32–35</sup> In addition, the constancy of the number and distribution of nuclei in the gel matrix implies that rates of crystallization of zeolites A and X are determined by the rates of their crystal growth, and thus, according with Eq. (2), by the concentrations of aluminum and silicon in the liquid phase.

Figure 3 shows that depending on the system, the concentration of aluminum,  $c_{\text{Al}}$ , in the liquid phase is approximately constant, or decreases slowly during the main part of the crystallization process, drops suddenly at the end of the crystallization process, and then gradually decreases until the equilibrium concentration,  $c_{\text{Al}} = c_{\text{Al}}(\text{eq})$  is

reached (symbols  $\circ$  and solid curves in Figures 3a–3g). For the »excess« of silicon in the liquid phase, *i.e.*,  $c_{\text{Si}} > c_{\text{Al}}$  (systems  $\emptyset$ , S1, S2, and S3),  $c_{\text{Al}}(\text{eq}) = c_{\text{Al}}^*$ , *i.e.*, aluminium concentration in the liquid phase which corresponds to the solubility of zeolite A crystallized under the given synthesis conditions.<sup>36</sup>

On the other hand, the concentration of silicon,  $c_{\text{Si}}$ , in the liquid phase is approximately constant during the »induction period« of the crystallization process, increases during the period of increased crystallization rate, reaches a maximal value at the end of the crystallization process, and then suddenly drops to any constant value  $c_{\text{Si}} = c_{\text{Si}}(\text{eq})$  (symbols  $\bullet$  and dashed curves in Figures 1b–7b). For the »excess« of aluminium in the liquid phase (systems A1, A2, and A3),  $c_{\text{Si}}(\text{eq}) = c_{\text{Si}}^*$ , *i.e.*, the concentration of silicon in the liquid phase that corresponds to the solubility of zeolite A crystallized under the given synthesis conditions.<sup>36</sup> The increase in  $c_{\text{Si}}$  during the period of increased crystallization rate is caused by the lower Si/Al ratio in the crystallized zeolite(s) (Si/Al = 1 for zeolite A, and Si/Al = 1.25 for zeolite X) than in the starting amorphous aluminosilicate precursor (= 1.32).<sup>11</sup> Since more than 90 % of Si and Al, respectively, is contained in the solid phase (aluminosilicate precursor), small differences of the general courses of the changes in  $c_{\text{Si}}$  and  $c_{\text{Al}}$  are probably caused by small variations of the Si/Al ratio in the precursor and the precursor content in the systems, respectively.<sup>11</sup>

The consequence of the decrease in the initial concentration of aluminium,  $c_0(\text{Al})$  (at  $t_c = 0$ ) in the liquid phase in the sequence:  $c_0(\text{Al})_{\text{A3}} > c_0(\text{Al})_{\text{A2}} > c_0(\text{Al})_{\text{A1}} > c_0(\text{Al})_{\emptyset} > c_0(\text{Al})_{\text{S1}} > c_0(\text{Al})_{\text{S2}} > c_0(\text{Al})_{\text{S3}}$ , and a simultaneous increase of the initial concentration of silicon,  $c_0(\text{Si})$ , in the liquid phase in the sequence:  $c_0(\text{Si})_{\text{A3}} > c_0(\text{Si})_{\text{A2}} > c_0(\text{Si})_{\text{A1}} > c_0(\text{Si})_{\emptyset} > c_0(\text{Si})_{\text{S1}} > c_0(\text{Si})_{\text{S2}} > c_0(\text{Si})_{\text{S3}}$  (see Figure 3) is an increase of the mole ratio  $R_c = c_0(\text{Si})/c_0(\text{Al})$  in the sequence:  $(R_c)_{\text{A1}} < (R_c)_{\text{A2}} < (R_c)_{\text{A3}} < (R_c)_{\emptyset} < (R_c)_{\text{S1}} < (R_c)_{\text{S2}} < (R_c)_{\text{S3}}$ . On the other hand, the approximate constancy of the product  $P_c = c_0(\text{Al}) \times c_0(\text{Si})$  indicates that the value of  $P_c$  is proportional to the solubility product of the amorphous aluminosilicate precursor in 1.4 M NaOH solution at 80 °C.

Figure 4 shows that the concentration factors,

$$f(c) = [c_{\text{Al}} - c_{\text{Al}}^*] [c_{\text{Si}} - c_{\text{Si}}^*]^r \quad (3)$$

( $r = 1$  for zeolite A, and  $r = 1.25$  for zeolite X) are linear functions of the crystallization time,  $t_c$ ,<sup>11,18,21</sup> *i.e.*,

$$f(c) = a + bt_c \quad (4)$$

up to the end of the crystallization process, suddenly drop thereafter due to the decrease in the aluminum and silicon concentrations in the liquid phase and converge to the value  $f(c) \rightarrow 0$  when  $c_{\text{Al}} \rightarrow c_{\text{Al}}^*$  (systems  $\emptyset$ , S1, S2 and S3; compare Figures 3e–3g and 4e–4g), and/or

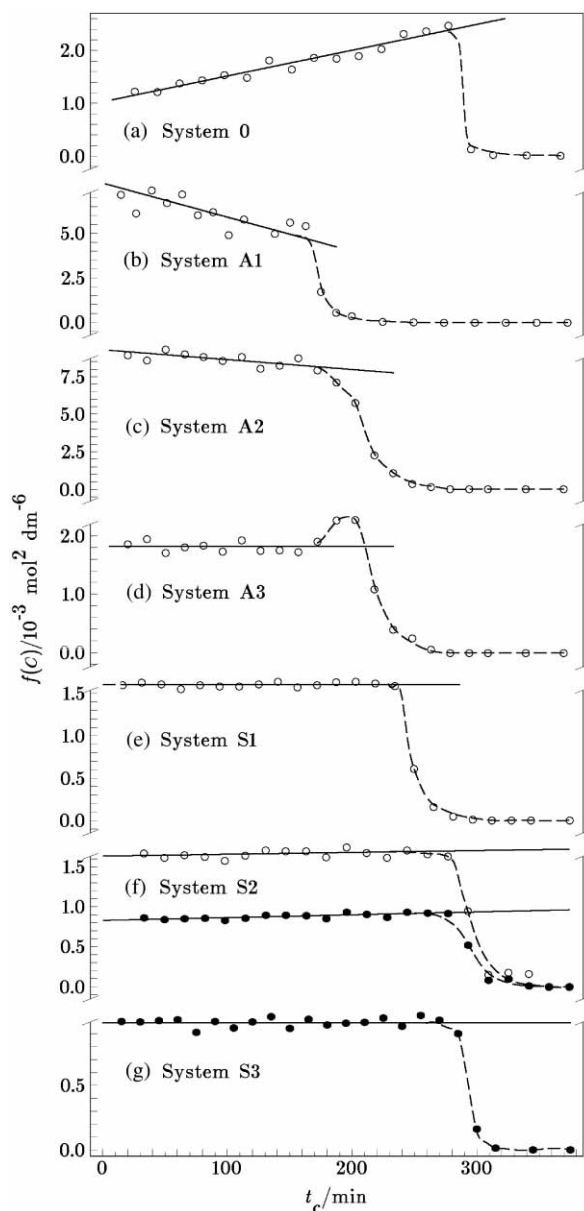


Figure 4. Changes in the values of concentration factors,  $f(c) = f(c)_{\text{A}}$  ( $\circ$ ), which correspond to the crystal growth of zeolite A, and  $f(c) = f(c)_{\text{X}}$  ( $\bullet$ ) which correspond to the crystal growth of zeolite X, during hydrothermal treatment of systems  $\emptyset$ , A1, A2, A3, S1, S2 and S3 at 80 °C. Solid curves represent the values of  $f(c)$  calculated by Eq. (4) using the corresponding values of  $a$  and  $b$  (Table V).

$c_{\text{Si}} \rightarrow c_{\text{Si}}^*$  (systems A1, A2, and A3; compare Figures 3a–3c and 4a–4c). The numerical values of constants  $a$  and  $b$  in Eq. (4), which correspond to the examined systems, are listed in Table V. According to Eq. (3), a combination of equations (2) and (4) gives:<sup>11,18,21</sup>

$$dL/dt_c = k_g (a + bt_c) \quad (5)$$

and thus,

$$L = k_g [at_c + b(t_c)^2/2] \quad (6)$$

TABLE IV. Values of the ratios  $R_c = c_0(\text{Si})/c_0(\text{Al})$  and products  $P_c = c_0(\text{Al}) \times c_0(\text{Si})$  of the initial concentrations of aluminum,  $c_0(\text{Al})$ , and of silicon,  $c_0(\text{Si})$ , in the liquid phase relevant for systems  $\emptyset$ , A1, A2, A3, S1, S2 and S3

System	$R_c$	$P_c / \text{mol}^2 \text{dm}^{-6}$
A3	0.139	0.00293
A2	0.332	0.00206
A1	0.476	0.00209
$\emptyset$	1.098	0.00184
S1	1.734	0.00209
S2	2.868	0.00202
S3	4.975	0.00193

The corresponding values of  $k_g$  were calculated as:<sup>11,18,21</sup>

$$k_g = L_m / [at_c + b(t_c)^2/2] \quad (7)$$

where  $L_m$  is the measured size of the largest crystals of zeolite A at the corresponding crystallization time  $t_c$  (symbols in Figures 1b and 1d). The average values of the constants,  $k_g$ , calculated in the above mentioned way, are in Figure 5 plotted against  $c_0(\text{Si})/c_0(\text{Al})$ . In addition, using the corresponding numerical values of the constants  $a$ ,  $b$  and  $k_g$ , the changes of  $L_m$  were calculated by Eq. (6) and correlated with the measured values of  $L_m$ . Figures 1b and 1d show that the calculated (curves) and the measured (symbols) changes of  $L_m$  are in excellent agreement in the time interval for which Eq. (4) is valid. This confirms the assumption that the crystal growth of zeolites A and X takes place according to the Davies and Jones model of growth and dissolution,<sup>19,20</sup> and thus that the rate of crystal growth depends on the concentrations  $c_{\text{Al}}$  and  $c_{\text{Si}}$ , as defined by Eq. (2), as previously confirmed by the analysis of the relationship between  $dL/dt_c$  and  $f(c)$  during the entire course of zeolite A crystallization.<sup>21</sup>

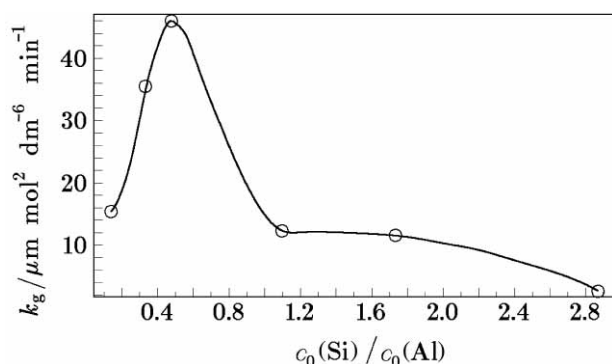
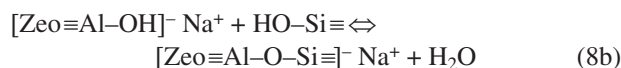
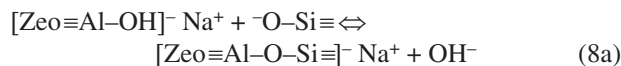


Figure 5. Influence of the starting mole ratio  $c_0(\text{Si})/c_0(\text{Al})$  of silicon and aluminum in the liquid phase on the value of the rate constant  $k_g$  of zeolite A crystals.

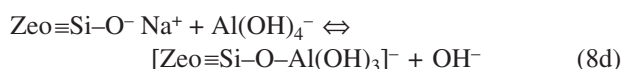
Lindner and Lechert<sup>37</sup> assumed that only monomeric silicate ( $\equiv\text{Si}-\text{O}^-$ ,  $\equiv\text{Si}-\text{OH}$ ) and aluminate ( $\text{Al}(\text{OH})_4^-$ ) species are responsible for crystal growth by nucleophilic attack on the aluminate centers ( $[\text{Zeo}\equiv\text{Al}-\text{OH}]^- \text{Na}^+$ ) at zeolite surface,



condensation reaction with a silanol group at the surface,



and incorporation of aluminium as a nucleophilic substitution reaction between deprotonated silanol groups on the surface and solvated aluminate species,



which at the same time explains why both concentrations of aluminium and silicon in the liquid phase influence the growth rate of aluminium-rich zeolites, in the simple way described by Eq. (2). In this context, the increase of the crystal growth rate of zeolite A in system A1 relative to system  $\emptyset$  was expected, due to the increase in the concentration of aluminate anions in the liquid phase and their role in the nucleophilic substitution reaction [see Eq. (8d)] as a determining step in the crystal growth process.<sup>13,37</sup> On the other hand, since

$$R_g = dL/dt_c = k_g f(c) = k_g (a + bt_c) \quad (9)$$

it is evident that the decrease of the value of  $k_g$  in the sequence:  $k_g(\text{A3}) < k_g(\text{A2}) < k_g(\text{A1})$  (see Figure 5), by an approximately constant value of  $R_g$  ( $= 0.028$  to  $0.034 \mu\text{m min}^{-1}$ ) (see Table II), is a consequence of the increase in the value of the concentration factor  $f(c)$  in the sequence:  $f(c)_{\text{A1}} > f(c)_{\text{A2}} > f(c)_{\text{A3}}$  (see Figure 4), caused

TABLE V. Numerical values of constants  $a$  and  $b$  in Eqs. (5) – (7)

System	$a / \text{mol}^2 \text{dm}^{-6}$		$b / \text{mol}^2 \text{dm}^{-6} \text{min}^{-1}$	
	zeolite A	zeolite X	zeolite A	zeolite X
$\emptyset$	$1.07 \times 10^{-3}$	–	$8.77 \times 10^{-6}$	–
A1	$7.78 \times 10^{-4}$	–	$-2.18 \times 10^{-6}$	–
A2	$9.25 \times 10^{-4}$	–	$-1.00 \times 10^{-6}$	–
A3	$1.82 \times 10^{-3}$	–	0	–
S1	$1.61 \times 10^{-3}$	–	0	–
S2	$1.64 \times 10^{-3}$	$8.30 \times 10^{-4}$	$2.50 \times 10^{-7}$	$3.83 \times 10^{-7}$
S3	–	$9.86 \times 10^{-4}$	–	0

by the increase in concentration  $c_{Al}$  relative to concentration  $c_{Si}$  (see Figure 3). This leads to the assumption that only selected (*e.g.*, monomeric and/or dimeric)<sup>3,11,13,18,37</sup> aluminate and aluminosilicate anions in the liquid phase participate in the crystal growth process in an »excess« of aluminium (systems A1, A2 and A3) and that this part of the aluminate and aluminosilicate anions are proportional to the entire amounts of silicate and aluminate ions present in the liquid phase, *i.e.*,

$$f(c)' = [f_{Al}(c_{Al} - c_{Al}^*)][f_{Si}(c_{Si} - c_{Si}^*)]^r = f_{Al} (f_{Si})^r f(c) \quad (10)$$

thus,

$$dL/dt_c = k_g f_{Al} (f_{Si})^r f(c) = k_g f_{Al} (f_{Si})^r (a + bt_c) \quad (11)$$

where  $f_{Al}$  and  $f_{Si}$  are fractions of the active aluminate, silicate and/or aluminosilicate anions that participate in the growth process, and  $f_{Al} (f_{Si})^r = \text{constant}$ . Validity of Eqs. (5) to (7) for the mathematical description of the linear part of crystal growth supports this assumption. A parallel change of constants  $R_g$  and  $k_g$  relevant for the growth of zeolite A crystals in systems Ø, S1 and S2 (see Table III) may be explained in the same way.

On the other hand, an increase in the concentration of silicon, and thus an increase of the ratio  $c_{Si}/c_{Al}$  in the liquid phase, increases the degree of polycondensation of silicate anions in the liquid phase, which favors zeolite X crystallization, and simultaneously lowers the possibility of zeolite A crystallization.<sup>1,18,32–35,38,39</sup> A small decrease of both rate constants,  $R_g$  and  $k_g$ , of the crystal growth of zeolite X with the increase of the mole ratio  $c_{Si}/c_{Al}$  in the liquid phase (see Tables II and IV and Figure 5) is caused by the decrease of the rate of nucleophilic substitution reaction [see Eq. (8d)] at a decreasing concentration of aluminate in the liquid phase.<sup>3,13</sup>

## CONCLUSION

Kinetics of both crystal growth and crystallization strongly depend on the concentrations of aluminium and silicon in the liquid phase of the crystallizing system. »Excess« of aluminium in the liquid phase increases both the rate of crystallization and the rate of the crystal growth of zeolite A relative to the reference system (no added »excess« of aluminate or silicate). On the other hand, the increase in the concentration (»excess«) of silicon in the liquid phase causes two effects: a decrease of the rates of both the crystallization and crystal growth of zeolite A and simultaneous crystallization of zeolites A and X. Moreover, zeolite X is the only product of crystallization from the system containing the largest amount of silicate.

Insensitivity of the particulate properties (crystal size distribution, average crystal size and specific number of zeolite crystals in the crystalline end products) to the excess of aluminate and silicate anions, respectively, in the

liquid phase, is in agreement with the »memory effect« of amorphous aluminosilicate precursors.

The linear relationship between the crystal growth rate,  $dL/dt_c$ , and the concentration factor  $f(c)$ ,  $dt_c = k_g f(c) = k_g [c_{Al} - c_{Al}^*][c_{Si} - c_{Si}^*]^r$  may be explained by the Davies and Jones model of dissolution and growth, which predicts formation of a monolayer of solvated ions of constant composition at the surface of the growing/dissolving crystals.

The size-independent crystal growth of zeolites A and X is governed by the reaction of monomeric and low-molecular aluminate, silicate and aluminosilicate anions from the liquid phase on the surfaces of the growing zeolite crystals, and hence only a part of aluminate and/or aluminosilicate anions in the liquid phase participate in the crystal growth process in the »excess« of aluminium; this part of aluminate and aluminosilicate anions are proportional to the entire amounts of silicate and aluminate ions present in the liquid phase.

Increase in the silicon concentration, and thus an increase of the ratio  $c_{Si}/c_{Al}$  in the liquid phase, causes an increase of the degree of polycondensation of silicate anions in the liquid phase, which favors zeolite X crystallization, and simultaneously lowers the possibility of zeolite A crystallization.

*Acknowledgement.* – This work was supported by the Ministry of Science and Technology of the Republic of Croatia.

## REFERENCES

1. B. Subotić, T. AntoniĆ, I. Šmit, R. Aiello, F. Crea, A. Nastro, and F. Testa, in: M. L. Occelli and H. Kessler (Eds.), *Synthesis of Porous Materials: Zeolites Clays and Nanostructures*, Marcel Dekker Inc., New York-Basel-Hong Kong, 1996, pp. 35–58.
2. S. P. Zhdanov and N. N. Samulevich, in: L. V. C. Rees (Ed.), *Proceedings of the Fifth International Conference on Zeolites*, Heyden, London-Philadelphia-Rheine, 1980, pp. 75–84.
3. A. Katović, B. Subotić, I. Šmit, L. J. A. Despotović, and M. Čurić, in: M. L. Occelli and H. E. Robson (Eds.), *Zeolite Synthesis*, ACS Symp. Ser. No. 398, American Chemical Society, Washington, DC, 1989, pp. 124–139.
4. T. AntoniĆ, B. Subotić, and N. Stubiĉar, *Zeolites* **18** (1997) 291–301.
5. S. P. Zhdanov, in: R. F. Gould (Ed.), *Molecular Sieve Zeolites I*, Advances in Chemistry Series, Vol. 101, American Chemical Society, Washington, DC, 1971, pp. 20–43.
6. H. Kacirek and H. Lechert, *J. Phys. Chem.* **79** (1975) 1589–1593.
7. H. Kacirek and H. Lechert, *J. Phys. Chem.* **80** (1976) 1291–1296.
8. H. Kacirek and H. Lechert, *J. Phys. Chem.* **80** (1976) 1291–1296.
9. B. Subotić and J. Bronić, in: R. von Ballmos, J. B. Higgins, and M. J. M. Treacy (Eds.), *Proceedings of the Ninth International Conference on Zeolites*, Butterworth-Heinemann, Boston, MA, 1993, pp. 321–328.

10. T. Antonić and B. Subotić, in: M. J. M. Treacy, B. K. Marcus, M. E. Bisher, and J. B. Higgins (Eds.), *Proceedings of the 12<sup>th</sup> International Zeolite Conference*, Material Research Society, Warrendale, PA, 1999, pp. 2049–2056.
11. S. Bosnar and B. Subotić, *Microporous Mesoporous Mater.* **28** (1999) 483–493.
12. S. Bosnar, J. Bronić and B. Subotić, in: I. Kiricsi, G. Pal-Borbely, J. B. Nagy, and H. G. Karge (Eds.), *Porous Materials in Environmentally Friendly Processes, Studies in Surface Science and Catalysis*, Vol. 125, Elsevier, Amsterdam, 1999, pp. 69–76.
13. B. Subotić, and J. Bronić in: S. M. Auerbach, K. A. Carrado, and P. K. Dutta (Eds.), *Handbook of Zeolite Science and Technology*, Marcel Dekker Inc, New York–Basel, 2003, pp. 129–203.
14. LJ. Brečević and D. Kralj, in: N. Kallay (Ed.), *Interfacial Dynamics*, Marcel Dekker, New York, 1999, pp. 435–474.
15. A. E. Nielsen, *Croat. Chem. Acta* **42** (1970) 319–333.
16. A. E. Nielsen, *Croat. Chem. Acta* **53** (1980) 255–279.
17. P.-P. Chiang and M. D. Donohue, *AIChE Symp. Ser.* **83** (1989) 28–36.
18. S. Bosnar, Ph.D. Thesis, University of Zagreb, Zagreb, 2000.
19. A. L. Jones and H. G. Linge, *Z. Phys. Chem. N.F.* **95** (1975) 293–296.
20. C. W. Davies and A. L. Jones, *Trans. Faraday Soc.* **51** (1955) 812–817.
21. S. Bosnar and B. Subotić, *Croat. Chem. Acta* **75** (2002) 663–681.
22. A. Katović, B. Subotić, I. Šmit, and LJ. A. Despotović, *Zeolites* **10** (1990) 634–641.
23. L. S. Dent Glasser, *Chem. Br.* (1982) 33–39.
24. J. Šefčik, Ph.D. Thesis, University of Minnesota, Minneapolis, 1997.
25. J. Šefčik and A. V. McCormick in: M. J. M. Treacy, B. K. Marcus, M. E. Bisher, and J. B. Higgins (Eds.), *Proceedings of the 12<sup>th</sup> International Zeolite Conference*, Material Research Society, Warrendale, PA, 1999, pp. 1595–1602.
26. J. Šefčik and A. V. McCormick, *Chem. Eng. Sci.* **54** (1999) 3513–3519.
27. L. S. Zevin and L. L. Zavyalova, *Kolichestvenniy Rentgenographicheskiy Prazoviy Analiz*, Nedra, Moscow, 1974, p. 37.
28. T. Antonić, Ph.D. Thesis, University of Zagreb, Zagreb, 1998.
29. T. Antonić-Jelić, S. Bosnar, J. Bronić, B. Subotić, and M. Škreblić, *Microporous Mesoporous Mater.* **64** (2003) 21–32.
30. T. Antonić and B. Subotić, in: *Zeolite Synthesis: From Dream to Production, Scientific Program of the 1<sup>st</sup> Euroworkshop on Zeolites*, Ronce-Les-Bains (La Rochelle), France, March 17–20, 1996, p. 33.
31. B. Subotić and T. Antonić, *Croat. Chem. Acta.* **71** (1998) 929–948.
32. M. Tatić and B. Držaj, in: B. Držaj, S. Hočevar, and S. Pejovnik (Eds.), *Zeolites: Synthesis, Structure, Technology and Application, Studies in Surface Science and Catalysis*, Vol. 24, Elsevier, Amsterdam, 1985, pp. 129–136.
33. E. I. Basaldella and J. C. Tara, *Zeolites* **15** (1995) 243–246.
34. Y. Traa and R. W. Thompson, *J. Mater. Chem.* **12** (2002) 496–499.
35. I. Krznarić, T. Antonić, J. Bronić, B. Subotić, and R. W. Thompson, *Croat. Chem. Acta* **76** (2003) 7–17.
36. A. Čizmek, LJ. Komunjer, B. Subotić, M. Široki, and S. Rončević, *Zeolites* **11** (1991) 258–264.
37. T. Lindner and H. Lechert, *Zeolites* **14** (1994) 582–587.
38. I. Krznarić, T. Antonić, B. Subotić, and V. Babić-Ivnančić, *Thermochim. Acta* **317** (1998) 73–84.
39. W. Wieker and B. Fahlke, in: B. Držaj, S. Hočevar, and S. Pejovnik (Eds.), *Zeolites: Synthesis, Structure, Technology and Application, Studies in Surface Science and Catalysis*, Vol. 24, Elsevier, Amsterdam, 1985, pp. 161–181.

## SAŽETAK

### Utjecaj koncentracije silicija i aluminija u tekućoj fazi na brzinu rasta mikrokristala zeolita A i X

Sanja Bosnar, Josip Bronić, Ivan Krznarić i Boris Subotić

Brzine rasta kristala zeolita A i X mjerene su tijekom kristalizacije pri 80 °C iz amorfnoalumosilikatnoga prekursora dispergirana u 1,4 M otopini NaOH koja je sadržavala različite količine otopljenoga NaAlO<sub>2</sub> ili Na<sub>2</sub>SiO<sub>3</sub>. Tijekom kristalizacije i frakcije zeolita A i X u produktima kristalizacije značajno ovise o sastavu tekuće faze kristalizacijskoga sustava. Analizom promjena koncentracija aluminija,  $c_{Al}$  i silicija,  $c_{Si}$  u tekućoj fazi te veličine  $L_m$ , najvećih kristala zeolita A i X tijekom kristalizacije, utvrđeno je da je brzina rasta kristala neovisna o njihovoj veličini te da se rast kristala odvija reakcijom monomernih i/ili niskomolekularnih aluminatnih, silikatnih i alumosilikatnih aniona iz tekuće faze na površini rastućih kristala zeolita. Utjecaj sastava tekuće faze kristalizacijskih sustava na tijek procesa kristalizacije i brzinu rasta kristala zeolita A i X razmatran je u odnosu na moguće raspodjele aluminatnih, silikatnih i alumosilikatnih aniona u tekućoj fazi.